Nonlinear mesoscopic transport in a strongly cooperative electron system: The $La_{0.67}Ca_{0.33}MnO_3$ microbridge

C. Beekman, J. Zaanen, and J. Aarts*

Kamerlingh Onnes Laboratorium, Leiden University, Niels Bohrweg 2, NL-2333 CA, Leiden, The Netherlands

(Received 6 March 2011; revised manuscript received 9 April 2011; published 14 June 2011)

We investigate the electrical transport in mesoscopic structures of $La_{0.7}Ca_{0.3}MnO_3$ in the regime of the metal-insulator transition by fabricating microbridges from strained and unstrained thin films. We measure current-voltage characteristics as function of temperature and in high magnetic fields. For strained films we find nonlinear effects in the steep part of the transition characterized by a differential resistance with a strong peak around zero applied current, and saturation at higher currents after a resistance drop of up to 60%. We propose that this nonlinear behavior is associated with the melting of the insulating state by injecting charge carriers, signaling the occurrence of an intervening phase that involves the formation of short-range polaron correlations.

DOI: 10.1103/PhysRevB.83.235128 PACS number(s): 75.47.Lx, 71.30.+h, 73.50.−h, 75.47.Gk

I. INTRODUCTION

Electrical transport on mesoscopic length scales has been extensively studied in weakly interacting electron systems but hardly in strongly correlated ones, although with their complex phases they can be expected to show novel physics. The challenge here is to prepare high-quality thin films of such materials and structure them in the micrometer regime. Below we report on the observation of a novel nonlinear transport phenomenon in microstructures consisting of a cooperative electron liquid, the current-driven melting of a polaron glass phase in microbridges of $La_{0.7}Ca_{0.3}MnO_3$ (LCMO). We find this effect precisely in the colossal-magnetoresistance (CMR) regime where the magnetoresistance is large and bulk measurements have established that the electron system is at least partially frozen into a polaron glass. Doped manganites such as LCMO are strongly correlated electron systems based on the insulating antiferromagnet $LaMnO_3$ showing a large variety in physical properties.[1,2] They come about by doping a 2^+ ion on the La^{3+} site, which leads to a mixture of charge and spin states (Mn^{3+} and Mn^{4+}). Since the Mn^{3+} ion is Jahn-Teller active, competing interactions are present: the trapping of electrons in Jahn-Teller (JT) distortions (lattice polarons), and the itinerancy of electrons combined with ferromagnetism through the double-exchange mechanism[3] when spins become polarized parallel to the core spins.

Generally, it is important to make the distinction between the material we are going to discuss, $La_{0.7}Ca_{0.3}MnO_3$, and materials which are specially tuned very close to an insulating phase. In the Ca-doped compound, the low-temperature d-electron bandwidth is small but present with a transition to a (lattice) polaron liquid at higher temperatures. In $Pr_{0.7}Ca_{0.3}MnO_3$, for instance, the metallic state never develops.[4] The tendency toward long-range charge order (CO) wins over band formation and the system stays insulating, although a magnetic field or even an electric field can still bring a ferromagnetic metallic state through a first-order "melting" transition.[5,6] These phase diagrams show that only small free-energy differences exist between the variety of different possible phases of the system. Tuning the chemical doping to almost insulating then leads to nanoscale phase separation as in the well-known example of $(La,Pr)_{0.6}Ca_{0.4}MnO_3$, where submicrometer coexistence of CO and FM states was found by electron microscopy.[7] It is mostly these systems where electrical transport on small length scales was probed in the regime of the metal-insulator (MI) transition.[8–10] Little work has been done on materials with larger bandwidths, e.g., LCMO, or on the question of nonohmic behavior in the CMR regime. Still, this is an issue in different fields. Dilute magnetic semiconductors such as (Ga,Mn)As are also showing signs of phase-separated ferromagnetic and paramagnetic regions and physics strongly similar to that of the manganites.[11] Understanding mesoscopic electrical transport in such complex systems is what we address.

We investigate microbridges with a width of a few micrometers made in LCMO thin films and grown strained or unstrained on $SrTiO_3$ (STO) or $NdGaO_3$ (NGO) substrates. Bulk LCMO shows an MI transition around $T_{MI} = 250$ K. Strain has an inhibiting effect on band formation, which leads to a reduction of T_{MI} compared to the bulk value,[12,13] which in the thinnest films goes down to 110 K. We can still vary this value, however, by making use of the fact that T_{MI} is higher when the film is grown on misoriented substrates. For an STO(001) substrate with a misorientation of 1° in the (100) direction, strain is still present but we find that $T_{MI} \approx 150$ K.[14] Such films were also investigated. In the strained microstructures, both on flat STO and misoriented STO, we find strongly nonlinear transport behavior in the CMR regime near the MI transition characterized by increased conductance at a higher current. We attribute this to the melting of a glassy polaron state, which forms when going from the correlated metal to the polaronic liquid.

II. EXPERIMENTAL METHODS

LCMO thin films with thicknesses between 7–20 nm were grown by dc sputtering in an oxygen atmosphere of 3 mbar and at a growth temperature of 840 °C, similar to a previous report.[12,15] The substrates were $SrTiO_3$(001) both flat and misoriented by 1° (with a cubic lattice and the lattice parameter $a_0 = 0.391$ nm) and $NdGaO_3$(100) (with a pseudocubic notation and $a_0 = 0.387$ nm).[16] Therefore, an LCMO film (with $a_0 = 0.386$ nm) undergoes a tensile strain of 1.3 or 0.3% when grown on STO or NGO, respectively.

Some of the misoriented substrates were treated in order to have a TiO_2 (singly) terminated surface. Transmission-electron microscopy showed all films to have the bulk *Pnma* structure. The thickness was checked by x-ray small-angle reflectivity measurements. Electron Energy Loss Spectroscopy (EELS) was used to characterize the elemental composition and the Mn valence state of the samples and showed that our films have compositions close to that of the sputtering target and correct oxygen stoichiometry.[14] The films were patterned using electron-beam lithography and Ar-etching followed by an oxygen plasma etch to restore the insulating properties of the substrate.[17] The mesoscopic LCMO structure has a four-point configuration of 5 μm width and 20–30 μm between voltage contacts, as shown in Fig. 1(a). Macroscopic Au/MoGe contacts were fabricated in a second e-beam step. We measured I-V curves as function of temperature and in high magnetic fields using a Physical Properties Measurement System (Quantum Design) for temperature and magnetic-field control (T = 20–300 K, H_a = 0–9 T), with an external current source and a (nano)voltmeter (in this case, Keithley 2182 with an internal resistance >10 GΩ was used) in order to increase the dynamic range of the measurements. Still, at the highest resistance the current source was voltage limited for strong currents. The magnetic field was always oriented perpendicular to the surface of the film. For later reference, note that the self-field of a current of 1 μA through a bridge of 1 μm is of the order of 10^{-6} T and hence incapable of producing any magnetoresistance effect.

III. RESULTS

A. Films on flat STO and NGO

I-V characteristics (by varying the current) were measured to determine the differential resistance (dV/dI) and the magnetoresistance (MR) between 20 and 300 K. Figure 1(b) shows the resistance versus temperature [$R(T)$] of a microbridge on a flat STO measured at currents of 100 nA (with current density $J = 2 \times 10^6$ A/m^2) and 2 μA (with $J = 4 \times 10^7$ A/m^2). Both sets of data show a clear MI transition typical for strained

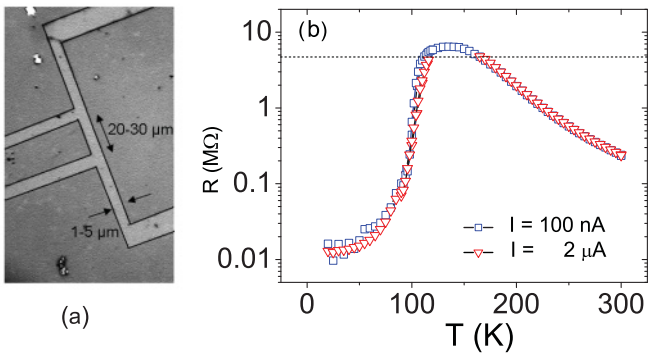

FIG. 1. (Color online) (a) Typical microbridge (an electron microscopy picture). The bridge width is 5 μm. (b) $R(T)$ at two different current densities [$J = 2 \times 10^6$ A/m^2 (squares) and $J = 4 \times 10^7$ A/m^2 (triangles)] for the 10-nm-thick bridge on a flat STO in a logarithmic scale. The dashed line indicates the measurement limit for the high-J measurement. The absence of resistance values above this limit is due to saturation of the nanovoltmeter.

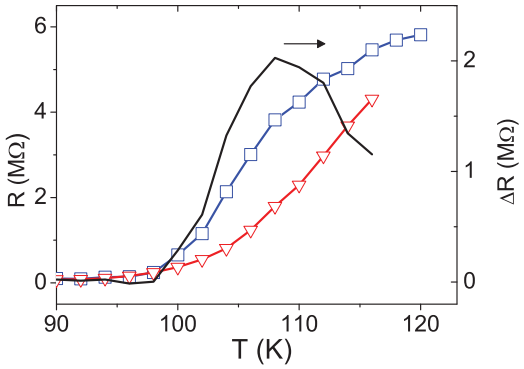

FIG. 2. (Color online) $R(T)$ between $T = 90$ and 120 K at two different current densities [$J = 2 \times 10^6$A/m^2 (squares) and $J = 4 \times 10^7$ A/m^2 (triangles)] for the 10-nm-thick bridge on a flat STO (left axis). Right axis and solid line represent the difference $\Delta R = R(100\text{nA}) - R(2\mu\text{A})$.

LCMO thin films with $T_{MI} = 130$ K (i.e., a peak temperature) and a resistance drop of three orders of magnitude.

In the logarithmic plot the difference between the two current values is not clearly visible and Fig. 2, therefore, displays $R(T)$ between 90 and 120 K on a linear scale. The plot shows that the difference is actually quite big. The higher current density results in a reduction of resistance just below T_{MI}, which produces a shift in the upper part of the transition of 5 to 10 K. Also shown is the difference between the two curves, which peaks between 105 and 110 K. If we define a current-induced electroresistance (ER) as ER(%) = $\frac{R_{high} - R_{low}}{R_{low}} \times 100\%$, then we observe a maximum ER effect of up to 60% for the 10-nm microbridge. The differences, of course, stem from the nonlinear behavior of the I-V curves, which is only found in the steep part of the transition. For other temperatures and for microbridges on NGO at all temperatures, the behavior is Ohmic.

Typical nonlinear behavior is shown in Fig. 3. The left panel shows dV/dI for the 10-nm microbridge at four different temperatures in 0-T field as a function of applied current density (bottom axis) and also as a function of the measured potential difference (V_m) between the voltage contacts (top axis). At low temperatures all I-V curves are linear up to $J = 8 \times 10^7$ A/m^2 ($I = 4\mu$A). Upon warming into the transition the nonlinear behavior starts to occur just below 96 K and appears to continue until T_{MI}. For all microbridges the differential resistance is the largest at zero bias and drops with increasing applied current density. The full width of the peak appears to increase by more than an order of magnitude from about 2×10^6 A/m^2 (0.2 V) at 96 K up to 4×10^7 A/m^2 (8 V) at 110 K. However, due to the voltage limit of the nanovoltmeter, it is difficult to observe any nonlinear behavior between 110 and 170 K. Above 170 K all I-V curves are linear. The right panel shows that applying a 5-T magnetic field leads to a reduction in the differential resistance and to complete disappearance of the nonlinearities in the I-V curves; they are linear across the entire temperature range. To compare the differential resistance behavior of different microbridges, we show dV/dI (see Fig. 4) normalized to the value at zero bias as a function of J for three microbridges on STO with different

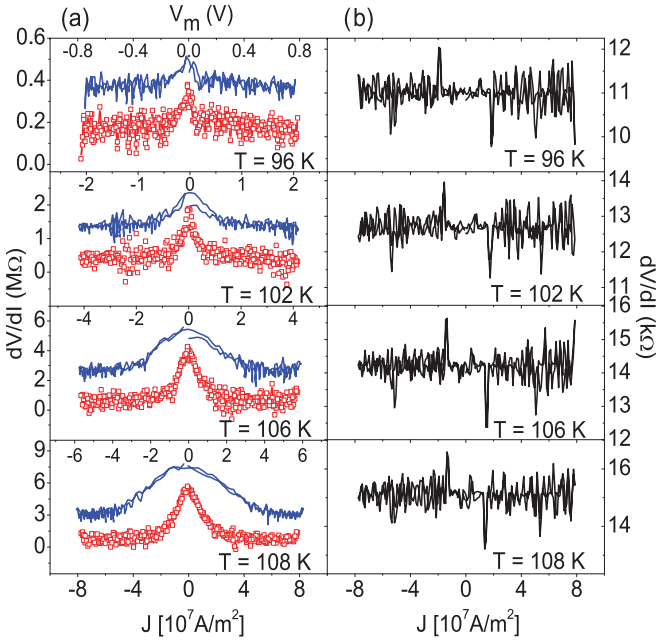

FIG. 3. (Color online) Numerical derivatives of the I-V data for the 10-nm-thick microbridge on a flat STO at four different temperatures [for the $R(T)$ behavior see Fig. 1(a)]. (a) Data for 0-T field. The bottom axis shows current density J (red squares), the top axis gives the measured potential difference (V_m) (solid blue line). (b) Data for 5-T field. The spikes are due to instrumentation.

thicknesses and at a temperature where the largest reduction occurred as a function of J.

The variation in dV/dI with J becomes less strong when the microbridge thickness is increased. Also shown in Fig. 4 are data for a 10-nm LCMO film grown on NGO (T_{MI} = 165 K) measured at 150 K, again, in the steep part of the transition. Although measured in a somewhat smaller current-density range we find no nonlinear behavior in films on NGO for thicknesses down to 10 nm.

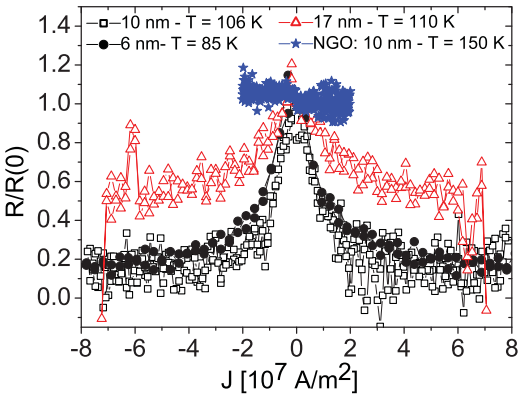

FIG. 4. (Color online) Numerical derivatives dV/dI of the I-V curves for three different bridges on a flat STO. The curves are normalized with respect to the zero-bias resistivity [17 nm: $R(0) = 0.3$ MΩ; 10 nm: $R(0) = 4.0$ MΩ and 6 nm: $R(0) = 4.3$ M]. Film thicknesses and the temperature of the I-V measurements are indicated. Also shown is the dV/dI at 150 K of the 10-nm LCMO film on NGO, which does not show nonlinear behavior.

Besides the well-known CMR effect in the transition, we also observe a strong MR effect at low temperatures for both microbridges on STO and NGO. As becomes clear from Fig. 5(a) this effect depends on the microbridge thickness. For the 17-nm-thick bridge the $R(T)$ curves at 0- and 5-T fields almost overlap but for the 10-nm-thick bridge a high magnetic field induces a significant reduction in R at low T. The magnitude of the low-temperature MR increases with reduced film thickness reaching about an order of magnitude for the 6.4-nm-thick film [see Fig. 5(b)]. Furthermore, also the (unstrained) 10-nm-thick film on NGO shows an MR effect of 50% at low temperatures. Apparently, even for the unstrained LCMO microbridge an applied magnetic field can result in increased metallicity at low T. On the other hand, we want to emphasize that in this regime of enhanced MR, the I-V characteristics are simply Ohmic.

B. Films on misoriented STO

Another set of measurements was performed on films grown and structured on STO with a misorientation of 1° to the (001)-surface normal and with a TiO_2 termination. Figure 6 shows the expected behavior in both 0- and 5-T fields with the MI transition at 160 K.

In this sample, nonlinear I-V characteristics are observed in a temperature range between 110 and 140 K. Examples of the differential resistance behavior are given in Fig. 7. The nonlinearities are found lower in the transition and the effect is smaller (by about 15%) but otherwise the behavior looks similar to that found in the structures on flat substrates. Also, the nonlinear behavior disappeared in the 5-T field.

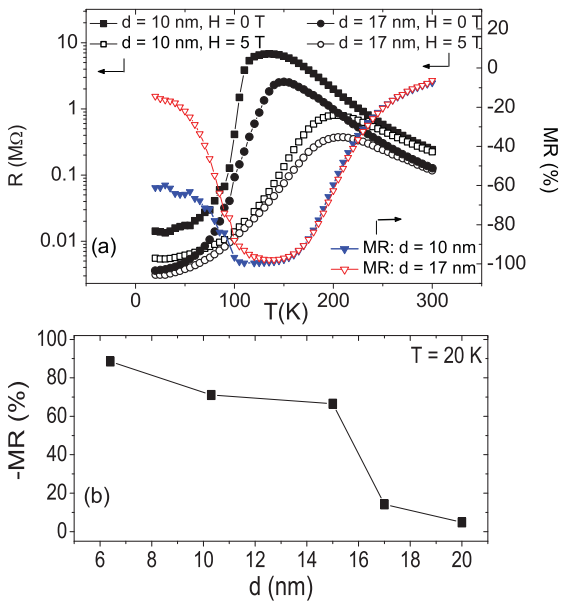

FIG. 5. (Color online) (a) $R(T)$ behavior in 0- and 5-T fields of a 17-nm-thick and 10-nm-thick microbridge. The calculated magnetoresistance as a function of temperature is also shown. (b) The calculated magnetoresistance [$MR(\%) = (R_{5T} - R_{0T})/R_{0T} \times 100\%$] as a function of the film thickness at $T = 20$ K.

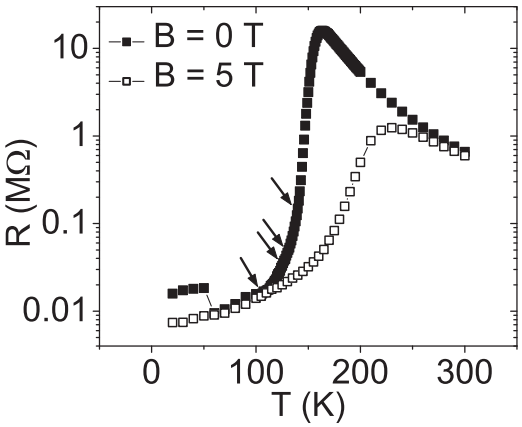

FIG. 6. $R(T)$ behavior in 0- and 5-T fields of a 10-nm-thick, 1-μm-wide microbridge grown on 1° misoriented STO. The measurement current was 0.5 μA (with $J = 1 \times 10^7$ A/m^2). Arrows denote the temperature regime where nonlinear I-V characteristics are observed.

IV. DISCUSSION

The behavior that was found here has not been reported before. Work on materials such as (La,Pr,Ca)MnO_3 was alluded earlier[8–10] and, basically, was focused on finding tunnelling phenomena due to the strongly insulating nature of some parts of the mixed phase, but never on finding a current-induced conductance increase. Our observations are not an artifact caused by Joule heating in the microbridge because by estimating the power inserted into the bridge from the peak resistivity (around $\rho \sim 10^5$–10^6 $\mu\Omega$ cm) and the relevant current densities we find values of the order of a few μW; the estimated Joule heating would have been then in the mK range, which is clearly negligible. Furthermore, heating would lead to a different nonlinear behavior, namely, *increase* of the resistance with increasing current. Such increase was actually found in thick unstructured LCMO films at a high current density together with heating-induced hysteretic behavior.[18] We find no hysteretic behavior either, which confirms that we can rule out heating in our case.

Another concern could be the influence of the structural phase transition, tetragonal to cubic, which occurs in the STO substrate at $T = 105$ K.[19,20] This phase transition has been studied extensively for both single crystals and thin films and is also known to depend on electric fields.[21,22] A shift of 10 K requires around 15 kV/cm. For the electric fields that we used (maximum at around 10^5 V/m), it is expected at 105 K and we have actually seen small resistance variations at this temperature in a 20-nm film, where R is already quite small itself. However, the fact that we have films (on a flat and misoriented STO), where the nonlinear behavior occurs at different temperatures but always in the region of the MI transition, rules out the phase transition as the origin of the observations and indicates that the nonlinear behavior is intrinsic to the material LCMO.

We conclude from this that the nonlinear behavior has to be the fingerprint of an organized phenomenon intrinsic to the electron matter formed in the manganite. Next, we discuss the different states of the microbridge as it is warmed through the MI transition. In Fig. 8, we provide the $R(T)$ data of the 10-nm microbridge on a flat STO, again, in order to identify the various regimes. At low temperatures (region I), the strong MR effects show that a high magnetic field can still assist in increasing the metallicity of the microbridge. We believe this is derived from static inhomogeneities, which lead to a relatively high residual resistance in the thinnest films and locally frustrate the double-exchange-type metallic state which then forms easier in a (high) magnetic field. The effect is rather similar to the MR reported in Ref. [24] in thin $La_{0.8}Ca_{0.2}MnO_3$ film, which also exists down to the lowest temperatures.

Upon warming into the transition the conduction electrons become more localized with the JT splitting of the e_g levels

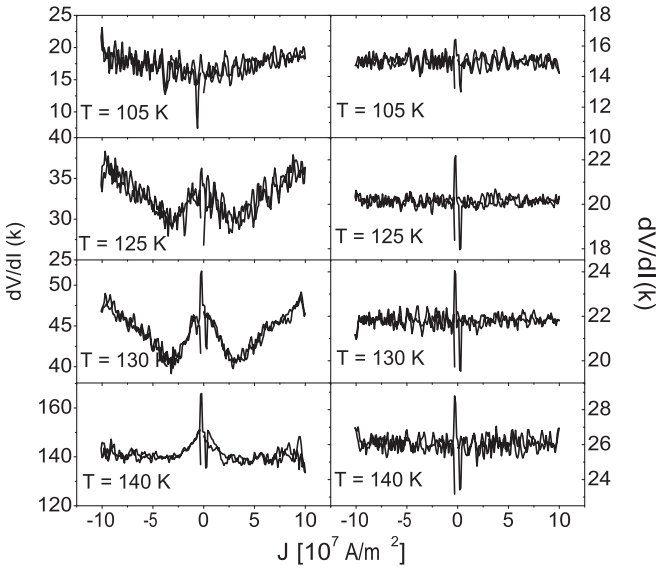

FIG. 7. Numerical derivatives of the measured I-V characteristics for the 10-nm-thick, 1-μm-wide microbridge grown on a 1°-misoriented STO at different temperatures (from top to bottom: 105, 125, 130, and 140 K). Panels on the left show data in zero field, panels on the right show data taken in 5-T field.

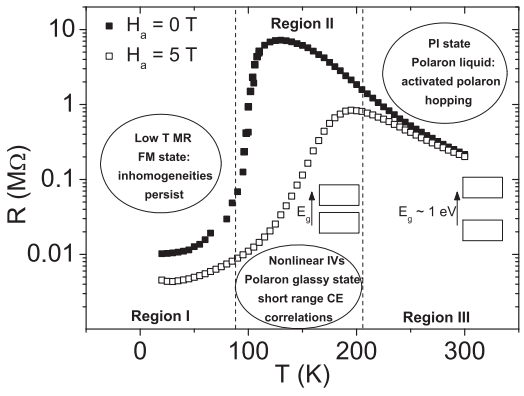

FIG. 8. Phase diagram for the 10-nm microbridge at low J. Region I: FM state with nanoscale inhomogeneities. Region II: e_g electrons are localized resulting in a glassy state of correlated (CE-type, charge-ordered) polarons. The I-V characteristics are nonlinear. Region III: the polaron correlations break down, the system becomes a polaron liquid with single dynamic polarons; the JT splitting, E_g, is of an order of 1 eV.[23]

assisted by the strain in the film leading to polaron formation. In the steep part of the transition, we begin to observe strongly nonlinear behavior and increasing conductance with current. The nonlinearities are fully reversible indicating that the process, which enhances the conductance, is not a first-order transition. A scenario in which current transforms a possible antiferromagnetic insulator to a ferromagnetic metal, e.g., through spin-torque processes, is not likely since the closeness of the MI transition in LCMO to a first-order transition[25] would probably render this process hysteretic. The scenario we propose instead is that the current-induced melting of an intervening phase, which can sustain a voltage difference while its electrical properties are extraordinarily sensitive to the injection of charge carriers, occurs in the high-current state. Such a phase could be the polaron-glass phase that was recently found by neutron-scattering experiments,[26] showing nanoscale structural correlations to occur just above T_{MI}. We can understand the origin of this phase by remembering that at a higher doping of $x \geqslant 0.5$, the material is antiferromagnetic and charge and orbital ordered. At the lower doping of $x = 0.33$, this ordering is frustrated but polaron correlations can still occur. The development of these static (charge-ordered, CE-type) polaron structures can trap electrons and drive the system into the insulating state. In our case, the correlated regions already start to occur below T_{MI} and become more abundant when the bridge is warmed through the transition, a process facilitated by the strain, which causes more disorder on nanoscales as well as larger JT distortions and smaller band widths. The resulting glass phase fully closes off the bridge, at least when the bridge is not too wide. The injection of carriers into this nascent state by applying a chemical potential difference works against the formation of the polaron correlations and drives the system to a different more metallic equilibrium. We note that the large CMR effect in the transition is itself related to the occurrence of the correlated polaron phase, as reported both experimentally[27,28] and theoretically,[29] while a similar scenario was suggested for the bilayer compound $La_{1.2}Sr_{1.8}Mn_2O_7$.[30] Warming into the region III, the polaron correlations break down (polaron liquid) and the conduction is governed by thermally activated (single-) polaron hopping.

In summary, we find that, upon reducing the size of a strained LCMO film grown on an STO substrate, novel behavior in the transport properties occurs, notably, nonlinear current-voltage characteristics. This is not found in wider bridges or when strain is absent (films on NGO). As a possible explanation we use the concept of a phase of glassy polarons, which is formed during the MI transition, assisted by the strain, and is very sensitive to the injection of charge carriers, leading to current-induced melting of the newly forming insulating state.

ACKNOWLEDGMENTS

We thank I. Komissarov for discussions, and M. Porcu and H. Zandbergen for the EELS measurements. This work was a part of the research program of the Stichting F. O. M., which is financially supported by NWO, and of the research program of the Dutch NanoNed consortium.

*aarts@physics.leidenuniv.nl

[1] *Colossal Magnetoresistive Oxides*, edited by Y. Tokura (CRC Press, Taylor & Francis, 2000).
[2] E. Dagotto, in *Nanoscale Phase Separation and Colossal Magnetoresistance*, Springer Series in Solid State Sciences Vol. 136 (Springer-Verlag, New York, 2003).
[3] C. Zener, Phys. Rev. **82**, 403 (1951).
[4] Y. Tokura, Y. Tomioka, H. Kuwahara, A. Asamitsu, Y. Moritomo, and M. Kasai, J. Appl. Phys. **79**, 5288 (1996).
[5] A. Asamitsu, Y. Tomioka, H. Kuwahara, and Y. Tokura, Nature (London) **388**, 50 (1997).
[6] Y. Tomioka, A. Asamitsu, H. Kuwahara, Y. Moritomo, and Y. Tokura, Phys. Rev. B **53**, R1689 (1996).
[7] M. Uehara, S. Mori, C. H. Chen, and S.-W. Cheong, Nature (London) **399**, 560 (1999).
[8] T. Wu and J. F. Mitchell, Phys. Rev. B **74**, 214423 (2006).
[9] H.-Y. Zhai, J. X. Ma, D. T. Gillaspie, X. G. Zhang, T. Z. Ward, E. W. Plummer, and J. Shen, Phys. Rev. Lett. **97**, 167201 (2006).
[10] G. Singh-Bhalla, S. Selcuk, T. Dhakal, A. Biswas, and A. F. Hebard, Phys. Rev. Lett. **102**, 077205 (2009).
[11] M. Sawicki, D. Chiba, A. Korbecka, Y. Nishitani, J. A. Majewski, F. Matsukura, T. Dietl, and H. Ohno, Nat. Phys. **6**, 22 (2010).
[12] J. Aarts, S. Freisem, R. Hendrikx, and H. W. Zandbergen, Appl. Phys. Lett. **72**, 2975 (1998).
[13] K. Dörr, J. Phys. D: Appl. Phys. **39**, R125 (2006).
[14] C. Beekman, M. Porcu, H. W. Zandbergen, and J. Aarts, e-print arXiv:1102.4004v1.
[15] Z. Q. Yang, R. Hendrikx, J. Aarts, Y. L. Qin, and H. W. Zandbergen, Phys. Rev. B **70**, 174111 (2004).
[16] NGO(100) is in pseudocubic notation. This is (110) in orthorhombic notation.
[17] C. Beekman, I. Komissarov, M. Hesselberth, and J. Aarts, Appl. Phys. Lett. **91**, 062101 (2007).
[18] Y. F. Chen and M. Ziese, J. Appl. Phys. **101**, 103902 (2007).
[19] K. A. Müller, W. Berlinger, and F. Waldner, Phys. Rev. Lett. **21**, 814 (1968).
[20] E. Courtens, Phys. Rev. Lett. **29**, 1380 (1972).
[21] K. C. Park and J. H. Choa, Appl. Phys. Lett. **77**, 435 (2000).
[22] D. C. Meyer, A. A. Levin, S. Bayer, A. Gorbunov, W. Pompe, and P. Paufler, Appl. Phys. A **80**, 515 (2005).
[23] M. Quijada, J. Cerne, J. R. Simpson, H. D. Drew, K. H. Ahn, A. J. Millis, R. Shreekala, R. Ramesh, M. Rajeswari, and T. Venkatesan, Phys. Rev. B **58**, 16093 (1998).
[24] M. Eblen-Zayas, A. Bhattacharya, N. E. Staley, A. L. Kobrinskii, and A. M. Goldman, Phys. Rev. Lett. **94**, 037204 (2005).
[25] D. Kim B. Revaz, B. L. Zink, F. Hellman, J. J. Rhyne, and J. F. Mitchell, Phys. Rev. Lett. **89**, 227202 (2002).

[26] J. W. Lynn, D. N. Argyriou, Y. Ren, Y. Chen, Y. M. Mukovskii, and D. A. Shulyatev, Phys. Rev. B **76**, 014437 (2007), and references therein.

[27] V. Kiryukhin, A. Borissov, J. S. Ahn, Q. Huang, J. W. Lynn, and S.-W. Cheong, Phys. Rev. B **70**, 214424 (2004).

[28] V. Moshnyaga, K. Gehrke, O. I. Lebedev, L. Sudheendra, A. Belenchuk, S. Raabe, O. Shapoval, J. Verbeeck, G. Van Tendeloo, and K. Samwer, Phys. Rev. B **79**, 134413 (2009).

[29] C. Sen, G. Alvarez, and E. Dagotto, Phys. Rev. Lett. **98**, 127202 (2007).

[30] N. Mannella, W. L. Yang, K. Tanaka, X. J. Zhou, H. Zheng, J. F. Mitchell, J. Zaanen, T. P. Devereaux, N. Nagaosa, Z. Hussain, and Z.-X. Shen, Phys. Rev. B **76**, 233102 (2007).